DOI: 10.1038/ncb2903

nature cell biology

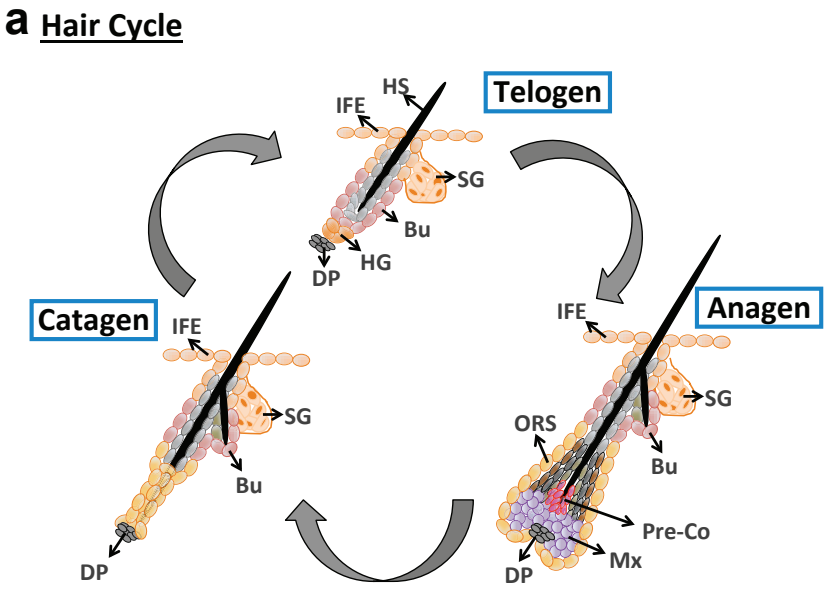

Supplementary Figure 1 Hair cycle (**a**) During the resting phase (telogen), HFSCs residing in the bulge (Bu) remain in quiescence as the terminally differentiated inner bulge cells express high levels of inhibitory signals (e.g. BMP, FGF18). At the onset of the regenerative phase (anagen), activated HFSCs located in hair germ (HG) proliferate and initiate HF regeneration in response to the activating cues (e.g. BMP inhibitors and Wnts) produced from crosstalk with the underlying mesenchymal stimulus, referred to as the dermal papilla (DP). Soon after, HFSCs in the bulge are also activated. Some activated HFSCs move downward from the bulge along the outer layer of HFs (ORS), creating an inverse gradient of proliferative cells that fuel the continued production of most proliferative, transient amplifying matrix cells (Mx) at the base of full anagen HFs. In response to high levels of Wnt signaling, matrix progenitors in the pre-cortex region (Pre-co) terminally differentiate to form the hair shaft (HS). At the end of anagen, HFs enter a destructive phase (catagen) and the matrix and much of the lower part of the HF undergo apoptosis. As the epithelial strand regresses, DP is drawn upward towards the bulge/HG and the HF re-enters telogen. IFE, interfollicular epidermis; SG, sebaceous gland.

a ***FACS scheme for isolating Wnt-responsive Bu-HFSCs (Axin2$^{LacZ/+}$)***

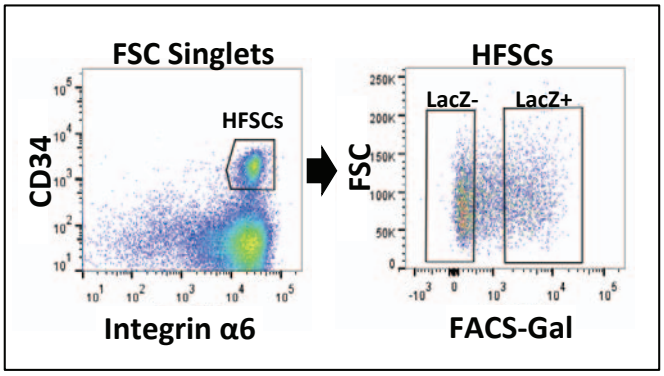

b ***HG cells at the bulge base are the first to proliferate at the telogen>anagen transition***

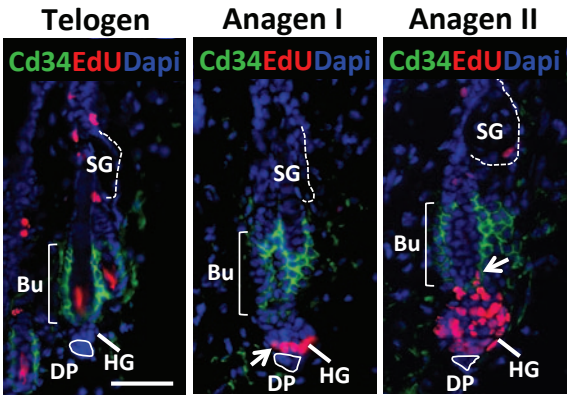

Supplementary Figure 2 Wnt-responsive Bu-HFSCs resemble HG HFSCs that first get activated and proliferate at the transition. (**a**) FACS-Gal sorting scheme to purify early anagen Bu-HFSCs. After sorting for Integrin α6 and CD34 surface expression, Bu-HFSCs were further fractionated into Wnt-responsive (LacZ+) and non-responsive (LacZ-) populations. (**b**) EdU and immunolabeling show that HG cells at the bulge base and in closest proximity to the dermal papilla (DP) stimulus, are the first to proliferate at the telogen→anagen transition. They expand and give rise to the transit-amplifying (TA) matrix; several days later, cells within the bulge begin to proliferate (arrow). Scale bar represents 50 μm.

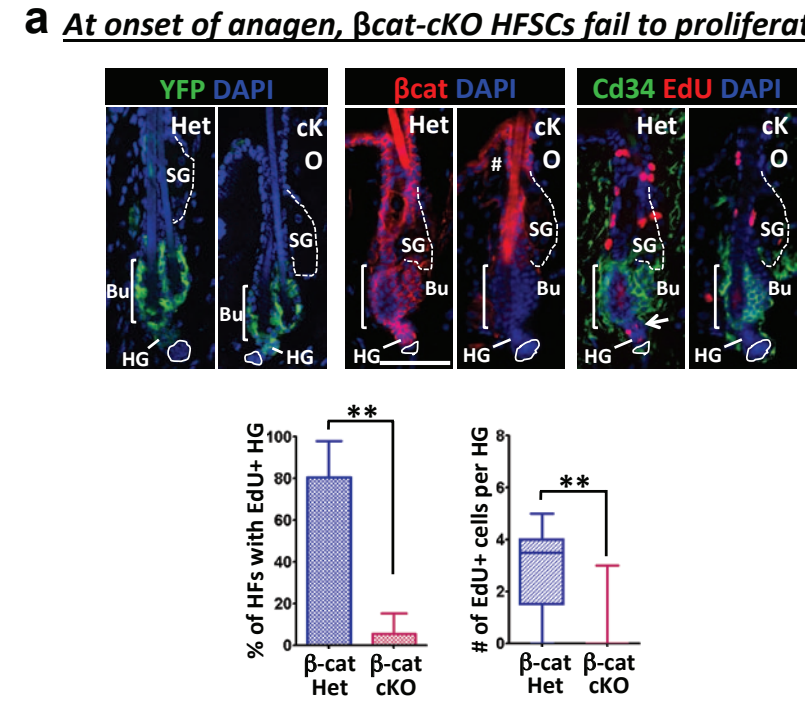

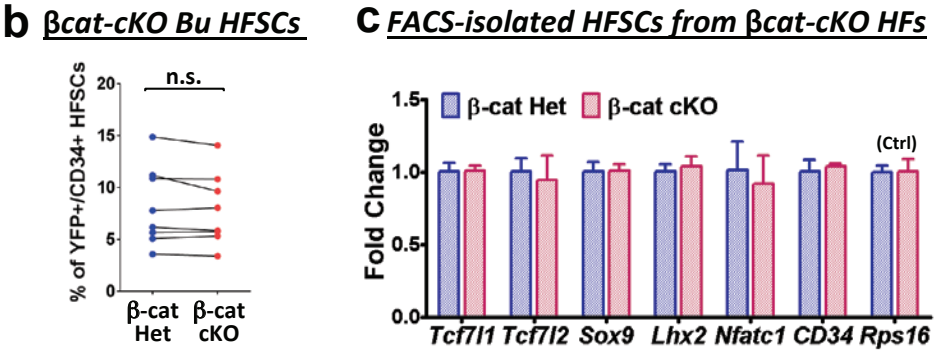

Supplementary Figure 3 YFP(+) βcat-cKO HFSCs fail to activate at anagen onset, but remain expressing HFSC stemness genes. (**a**) Immunolabelling shows that at telogen®anagen when the first sign of proliferation (arrow) is seen in YFP(+) control HGs, YFP(+) βcat-cKO HFSCs remain quiescent. Quantifications of EdU-labeling experiments are at bottom. Scale bar represents 50 µm. Data are reported as average + SD. n=3; **, p<0.01. (**b**) FACS analysis for YFP(+)/CD34(+) Bu-HFSCs reveals comparable percentages of control (β-cat Het) and βcat-cKO (β-cat cKO) Bu-HFSCs among HFs from eight different pairs of littermates. n=8; n.s., not significant. (**c**) Real-time PCR analysis for HFSC stemness genes. FACS-purified telogen-phase Bu-HFSCs from Het and βcat-cKO mice (10d post RU486-induced ablation). Values are normalized to β-cat Het Bu-HFSC mRNAs. Data are reported as average + SD. n=3. Error bars for qPCR calculated from technical triplicates. Similar results were reproduced in 3 independent experiments.

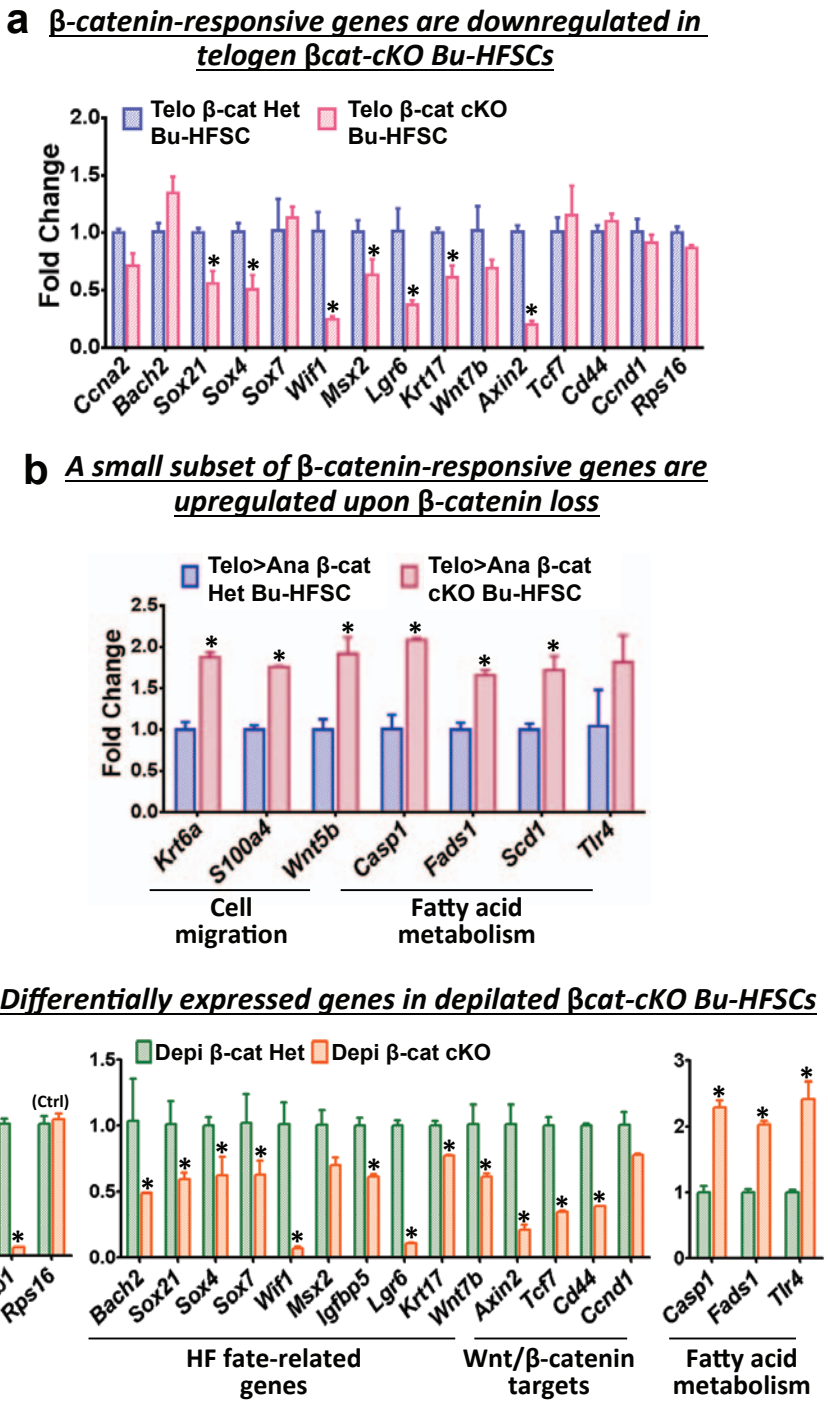

Supplementary Figure 4 Genes that are differentially expressed depending upon β-catenin status. (**a**) qPCR of telogen-phase Bu-HFSCs confirms RNA-seq data from Telo→Ana (see Fig. 5) showing that upon β-catenin ablation, a cohort of genes are also downregulated in quiescent Bu-HFSCs lacking β-catenin. (**b**) qPCR confirms that upon β-catenin ablation, a smaller subset of genes are upregulated at Telo→Ana within Bu-HFSCs. Note that fatty acid metabolism genes are elevated in βcat-cKO Bu-HFSCs. (**c**) Depilation-activated βcat-cKO HFSCs show similar gene changes to those seen in Fig. 5b and S4b. Values in (a)-(c) are normalized to β-cat Het Bu-HFSC mRNAs. Data are reported as average + SD. n=3; *, $p<0.05$. Error bars for qPCR calculated from technical triplicates. Similar results were reproduced in (a) 3, (b) 3 and (c) 2 independent experiments.

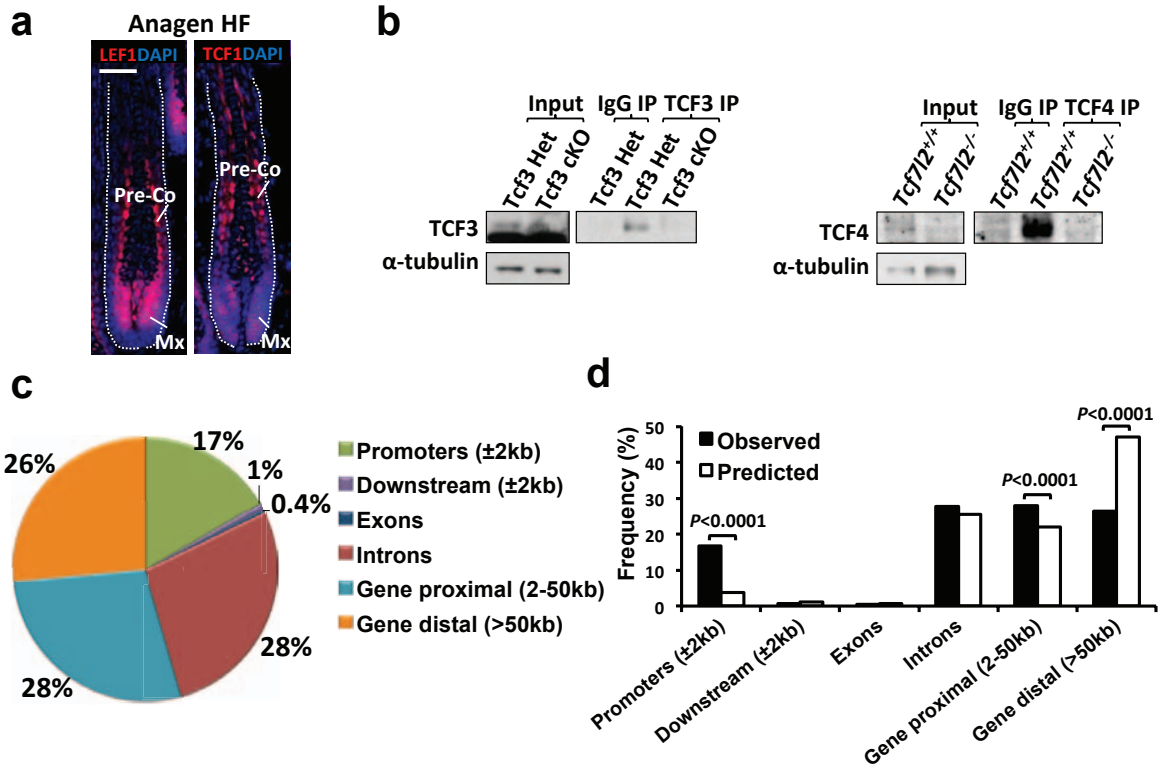

e TCF3/TCF4 co-peaks (±150bp, p<0.0005)

Motif Logo	Matching Known Motif	% of Peaks	% of Random Sequences	p-value (peaks vs random)
	LEF1/TCF	36	17	<2.2e-16
	N/A	10	4	<2.2e-16
	NFATc	25	15	<2.2e-16

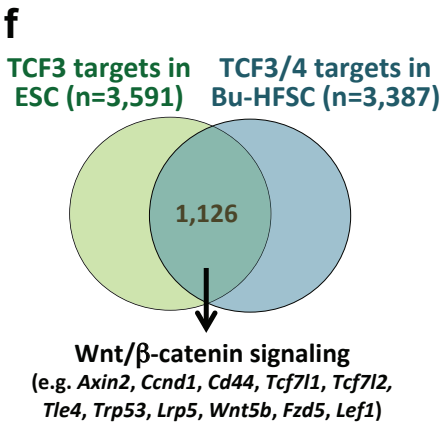

Supplementary Figure 5 TCF3 and TCF4 co-target genes. (**a**) LEF1 and TCF1 are expressed and nuclear in adult anagen HFs. Mx, matrix; Pre-Co, pre-cortex. Scale bar represents 50 μm. (**b**) The specificity and quality of TCF3 and TCF4 antibodies were validated by their pull-down ability in HFSC lysates relative to those pull-down with *Tcf7l1*-null or *Tcf7l2*-null skin cells, and to IgG controls. Immunoblotting analyses of immunoprecipitations reveal that sufficient amounts of TCF3 and TCF4 proteins in HFSC lysates were pulled down relative to IgG controls. (**c**) Genomic distribution of TCF3/4 ChIP-seq co-peaks relative to RefSeq transcripts. Promoter: within ±2kb of transcription start site. Downstream: within ±2kb of transcription end site. Gene proximal: within upstream 2-50kb of transcription start site. Gene distal: beyond upstream 50kb of transcription start site. (**d**) Comparison of the observed TCF3/4-bound peak distribution to the predicted distribution based on the genomic representation of each compartment. (**e**) Putative transcription factor binding motifs were discovered from *de novo* motif analysis using MEME-ChIP software[59]. The percentages of motif occurrences within TCF3/4-bound peaks versus random genomic sequences are indicated for each motif as determined by the program MAST (p<0.0005). *p*-values are determined by compared to the percentage observed in random sequences. In addition to Lef1/TCF motif, NFATc1 was the top known motif found at TCF3/4-bound peaks. (**f**) Most enriched gene ontology for the overlapping targets (n=1,126) of TCF3 targets in mESCs (n=3,591; green)[28], and TCF3/4 targets in HFSCs (n=3,387; blue).

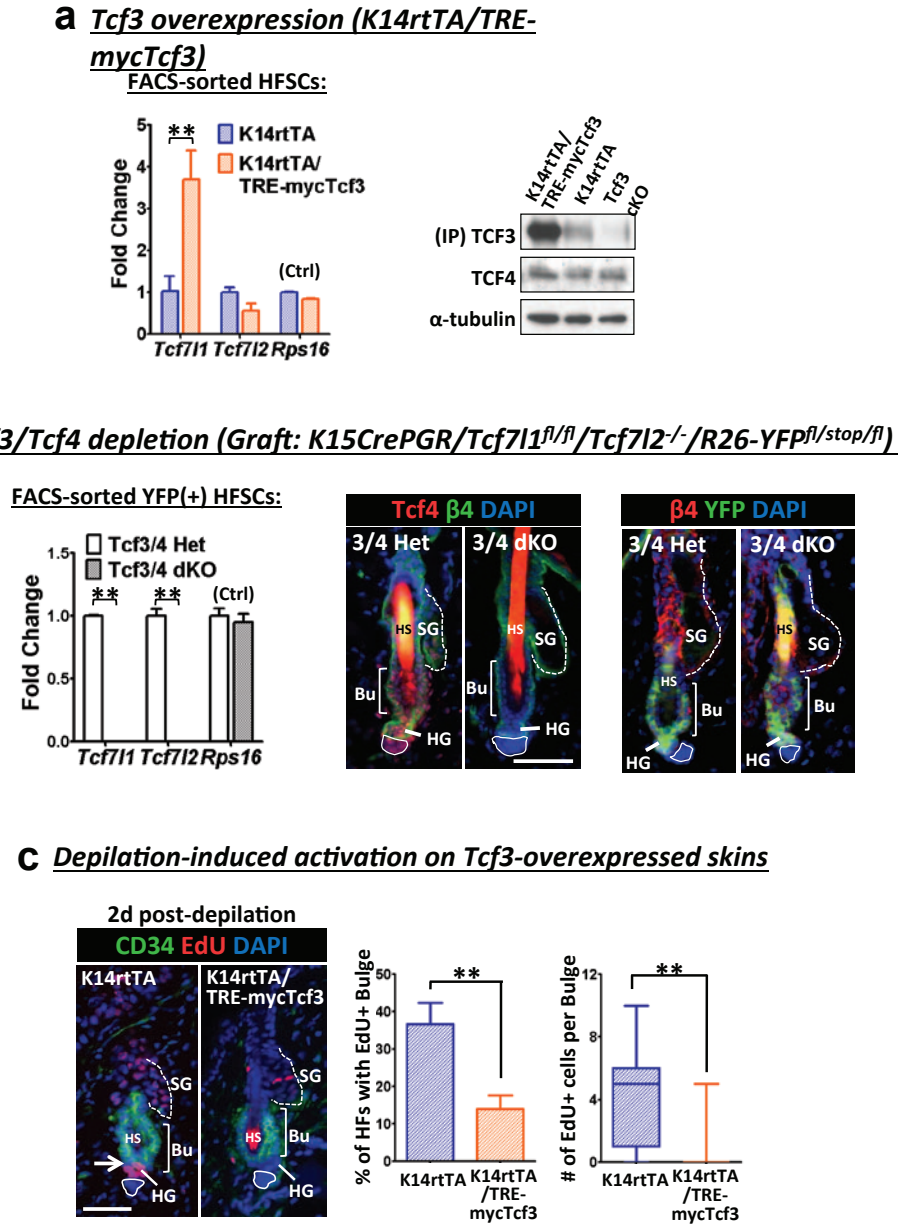

Supplementary Figure 6 Gain- and loss-of-function for TCF3 and TCF4. (**a**) TCF3 overexpression. qPCR (left) and immunoblotting (right) analyses showing elevated TCF3 mRNA and protein in Bu-HFSCs following Doxy induction of *K14rtTA/TRE-mycTCF3* mice. Values are normalized to *K14rtTA* Bu-HFSC mRNAs. *Rps16,* mRNA control; α-tubulin; protein loading control. (**b**) Depletion of TCF3 and TCF4 in HFSCs. E18.5 back skins of *K15CrePGR/Tcf7l1*$^{fl/fl}$*/Tcf7l2*$^{-/-}$*/Rosa26-YFP*$^{fl/stop/fl}$ embryos were grafted onto *Nude* mice, and 7 weeks later, when HFs were in telogen, RU486 was administered to generate double knockout (dKO) HFSCs. qPCR analysis with FACS-isolated Bu-HFSCs from RU486-treated *K15CrePGR/Tcf7l1*$^{+/fl}$*/Tcf7l2*$^{+/-}$*/Rosa26-YFP*$^{fl/stop/fl}$ (TCF3/4 Het) and *K15CrePGR/Tcf7l1*$^{fl/fl}$*/Tcf7l2*$^{-/-}$*/Rosa26-YFP*$^{fl/stop/fl}$ (TCF3/4 dKO) grafted skins. (Left) qPCR analysis demonstrates Tcf3 and TCF4 depletion. (Right) Immunostaining of grafts demonstrates Tcf4 depletion and Cre activation (YFP+). (**c**) Elevated TCF3 prohibits depilation-induced HFSC activation. Doxy was given throughout. One day after depilation, EdU was administered for 24 hours to identify proliferating cells. (Left) Immunostaining for EdU and Bu-HFSC marker CD34. (Right) Quantifications of EdU-labeling experiments. Note that HFs with increased TCF3 display reduced HFSC activation. Scale bars in (b) and (c) represent 50 μm. Data in (a)-(c) are reported as average + SD. n=3; **, p<0.01. Error bars for qPCR calculated from technical triplicates. Similar results were reproduced in (a) 5 and (b) 3 independent experiments.

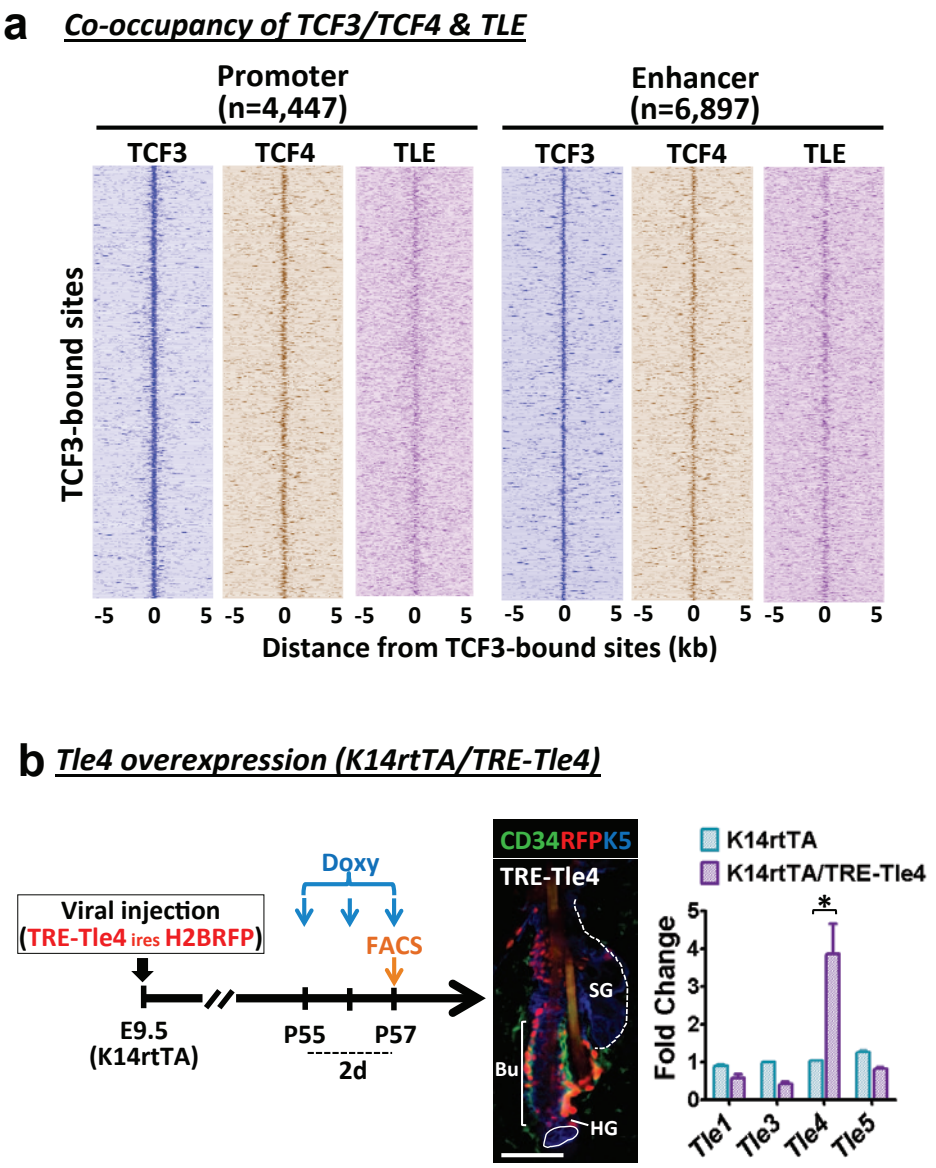

Supplementary Figure 7 Co-occupancy of TCF3, TCF4 and TLE in quiescent bulge HFSCs. (**a**) TLE occupies bulge HFSC DNA locations that are also bound by TCF3 and TCF4. Density maps of TCF3 (blue), TCF4 (orange), TLE (purple) ChIP-seq reads (x-axis, centered on TCF3 peak summits) at TCF3-bound peaks (Y-axis), broken into peaks in promoter and enhancer regions. (**b**) Overexpression of TLE4 in HFSCs. (Left) Lentiviral construct carrying Doxy-inducible *TRE-Tle4* and *H2BRFP* genes was introduced to E9.5 *K14rtTA* embryos by *in utero* infection[52], and at adulthood, Doxy was administered according to schematic. (Middle) A transduced (RFP+) HF. Scale bar represents 50 μm. (Right) qPCR analysis of FACS-isolated RFP(+) Bu-HFSCs from Doxy-induced mice. Note elevated *Tle4* mRNA levels relative to control. Data are reported as average + SD. n=3; *, $p<0.05$. Error bars for qPCR calculated from technical triplicates. Similar results were reproduced in 3 independent experiments.

Full Scan of immunoblots

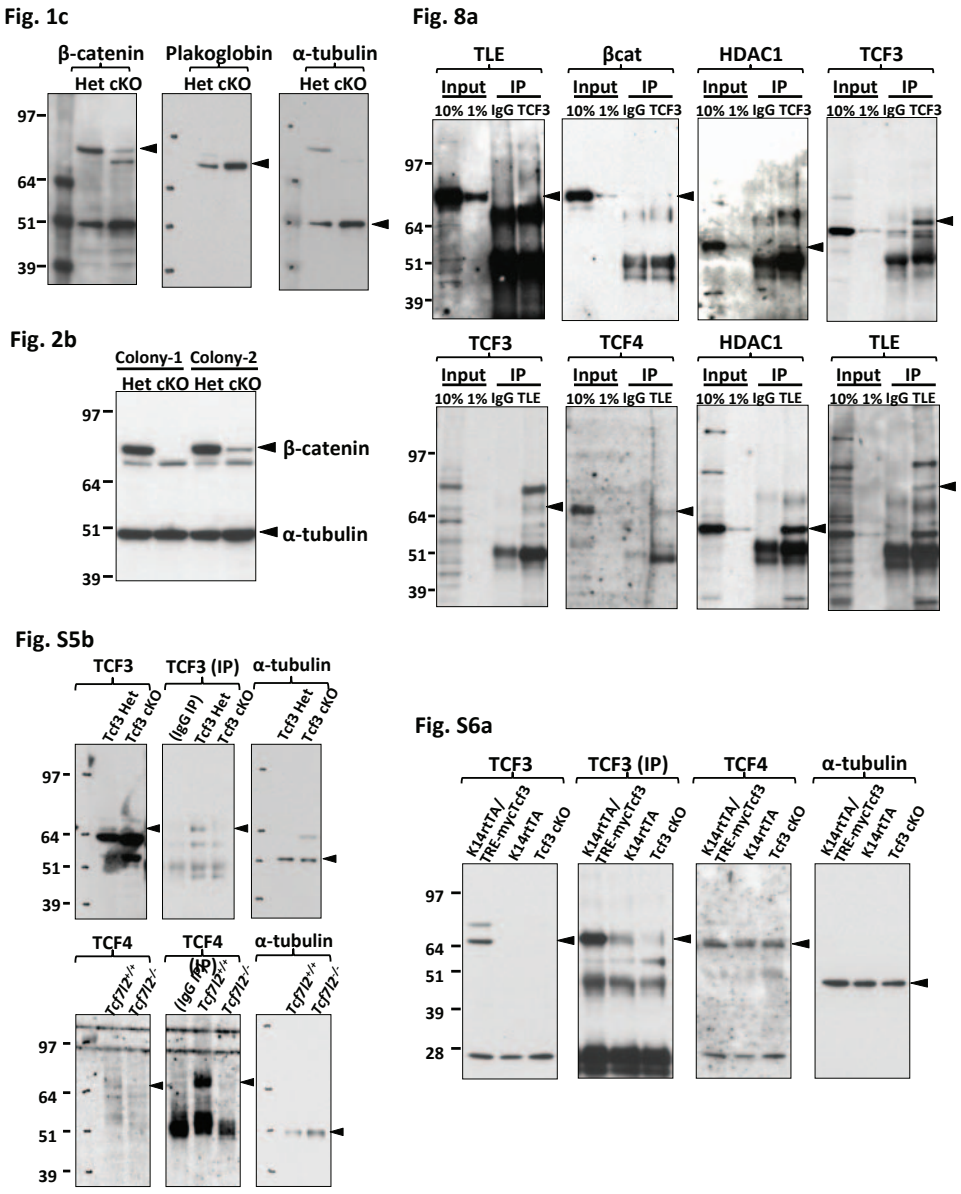

Supplementary Figure 8 Full scan of immunoblots. Full scan of cropped immunoblot images in Fig. 1c, 2b, 8a, S5b and S6a are shown.

Supplementary Tables

Table S1 Expression levels of TCF3/4 and β-catenin target genes in Wnt-responsive HFSCs. Lists of TCF3/4/β-catenin co-target genes that are bound (n=100) or not bound (n=35) by TLE while in telogen. Random selected TCF3/4-only targets that are bound (n=100) or not bound (n=100) by TLE as controls. Gene expression levels (FPKM) and fold changes in βcat-cKO (cKO) vs control (Het) Bu-HFSCs, and LacZ(+) vs LacZ(-) Bu-HFSCs from *Axin2*$^{LacZ/+}$ mouse are shown in a supplementary Excel file (Table S1).

Table S2 Primers used for mRNA expression. The sequences of primer sets used for qPCR analysis for mRNA expression are listed in a supplementary Excel file (Table S2).

Table S3 Primers used for ChIP-seq validation. The sequences of primer sets used for qPCR analysis for ChIP-seq validation are listed in a supplementary Excel file (Table S3).